Eur. Phys. J. A **11**, 403–411 (2001)

THE EUROPEAN PHYSICAL JOURNAL A

Covalently bound molecular structures in the $\alpha + {}^{16}$O system

W. von Oertzen[1,2,a]

[1] Freie Universität Berlin, Fachbereich Physik, Arnimallee 14, 14195 Berlin, Germany
[2] Hahn-Meitner-Institut Berlin, Glienicker Strasse 100, 14109 Berlin, Germany

Received: 11 July 2001
Communicated by P. Schwalm

Abstract. Using the concept of covalent molecular orbitals for neutrons and the known properties of the local $\alpha + {}^{16}$O potential the formation of *asymmetric molecular structures* in neon isotopes is discussed. Experimental evidence for parity doublets in ^{21}Ne is reviewed and a corresponding band structure for the states in ^{21}Ne at moderate excitation energy of $E_x = 0$–8 MeV is proposed. The structure of some bands can be interpreted as consisting of an instrinsic asymmetric (^{4}He + ^{16}O) structure bound by a covalent neutron in σ and π orbitals. An extension of the observed structures to *symmetric molecular structures* in isotopes of Mg and heavier nuclei is suggested. In particular shape isomers in isotopes of magnesium, namely $(He)_2O$ molecules, can be predicted and an *extended Ikeda diagram is proposed*.

PACS. 21.10.-k Properties of nuclei; nuclear energy levels – 21.60.Gx Cluster models

1 Introduction

The physics of molecular orbitals for nucleons (mostly neutrons) has been developed in the last decades and has been successfully applied in the description of transfer processes of neutrons and protons in heavy-ion reactions at low energy [1–8]. In these models valence particles and cores are defined, with the cores being typically strongly bound clusters. The valence nucleons move in the field of two clusters and some concepts of molecular physics with atoms (there named LCAO) can be applied. The method of linear combinations of nucleon orbitals (LCNO) to define the two-centre states has been used for cases with ^{12}C and ^{16}O cores, where the concept of strongly bound cores and loosely bound neutrons is applicable [2,4,5,7]. Also in nuclear-structure calculations this approach has been used to identify molecular structures in beryllium and boron isotopes [9]. In addition, this concept has been applied to α-cluster nuclei in ref. [10] for α-particles (called there again LCAO).

The concept of molecular orbitals has been used mainly in a *dynamical theory* to describe neutron transfer reactions between light nuclei in systems like ^{12}C + ^{13}C, ^{13}C + ^{14}C, ^{13}C + ^{13}C, ^{17}O +^{13}C, ^{17}O +^{16}O and others. The reaction calculations are performed in coupled reaction channel approaches, where the LCNO serves as an alternative (complete) set of basis states for transfer processes and the description of phenomena like Landau-Zener transitions and enhanced fusion processes can be achieved [2,4,5,11,6]. The validity of the adiabatic approximation has been demonstrated for many reactions at energies close to the Coulomb barrier involving low-lying scattering states. The condition for quasi-stationary (or stable) molecular states with long lifetime, where a repulsion occurs at smaller distances, is not fulfilled in these cases. The interaction potentials between the cores have usually been determined from the analysis of elastic scattering; in most cases they become strongly attractive once the Coulomb barrier has been passed. The strongly attractive mean-field potential between the two cores at small distances leads to a fusion process and to the formation of a compound nucleus.

Appropriate conditions for the formation of stable or quasi-stationary molecular states can easily be formulated. We need: a) strongly bound cores; b) a weakly attractive core-core potential which becomes repulsive at small distances; c) weakly bound single-particle orbitals of valence neutrons in order to guarantee large amplitudes of covalent particle wave functions at larger distances in the overlap region; d) large transfer probability, which is typically reached if the valence states are in the resonance or in a quasi-resonance matching condition between the two states of the separated centres.

The beryllium isotopes can be considered as well-established cases of covalently bound nuclear molecules [9, 12], where the two α-particles are bound by neutrons. This fact gives rise to very characteristic isomeric structures, which are based on the σ and π binding neutron orbitals constructed from the $p_{3/2}$ orbits in ^{5}He of the separated centres. This feature has also been well demonstrated

[a] e-mail: oertzen@hmi.de

by "model-independent" calculations using the method of Antisymmetrised Molecular Dynamics (AMD) of Kanada-En'yo and Horiuchi [13–15]. Pronounced molecular structures are observed a few MeV below the threshold for the decay into α-particles and neutrons. These states in the beryllium isotopes (^{9}Be, ^{10}Be and ^{11}Be) are dimers in the sense of the atomic molecules, with well-separated centres and molecular orbital structure for the valence particles. In addition to the Be isotopes, dimer structures have been identified in their isobaric analogue states —in the boron isotopes [12].

I will show in the present work that another favourable case for covalent molecular binding via neutron orbitals can be found in the $\alpha + {}^{16}$O system. In this case, the particular symmetry due to two identical cores, which occurs in the beryllium isotopes is not valid. Other characteristic symmetries of *intrinsically asymmetric* molecules will become apparent. These are discussed in the text books on molecular physics by Herzberg [16], and by Bohr and Mottelson [17] for nuclei with intrinsic octupole deformation. A more general discussion of reflection asymmetric shapes in nuclei up to the heaviest elements has been given by Butler and Nazarewicz in ref. [18].

I will restrict myself to the detailed discussion of possible evidence for molecular structure in ^{21}Ne, which can serve as a building block for molecules based on the $\alpha + {}^{16}$O clustering, and related to the instrinsic octupole shape of this two-cluster system. In sect. 2 the structure of ^{20}Ne is shortly reviewed, which will show a coexistence of quadrupole deformed bands with those based on the $\alpha + {}^{16}$O cluster structure; section 3 gives a discussion of the possible molecular wave functions of some states in ^{21}Ne. The available information on the structure of ^{21}Ne is used to build rotational bands, which will give evidence for molecular structures. Based on these results, strongly deformed molecular states can be predicted in other neutron-rich isotopes of neon, magnesium and in heavier nuclei at excitation energies close to the thresholds for the decomposition into clusters plus covalent neutrons, in close analogy to the Ikeda diagram [19,20]. In sect. 4 possible alternative interpretations in the framework of the deformed shell model (Nilsson model) are shortly discussed. In sect. 5 molecules in the form of $(He)_2O$ (which could be named *"nuclear water"*) or $(O)_2He$ are proposed, as well as other structures based on the covalent neutron bonds and the $\alpha + {}^{16}$O potential. The results will allow the design of an "extended Ikeda" diagram.

2 Structure of the neon isotopes $^{20-21}$Ne and the $\alpha + {}^{16}$O potential

2.1 Structure of ^{20}Ne

The scattering of α-particles on ^{16}O has been the subject of intense study up to the recent years. I refer as a survey to the work of Ohkubo *et al.* [21]. There, it is shown that a shallow local potential, which is phase equivalent to the deep potential obtained in a double-folding model,

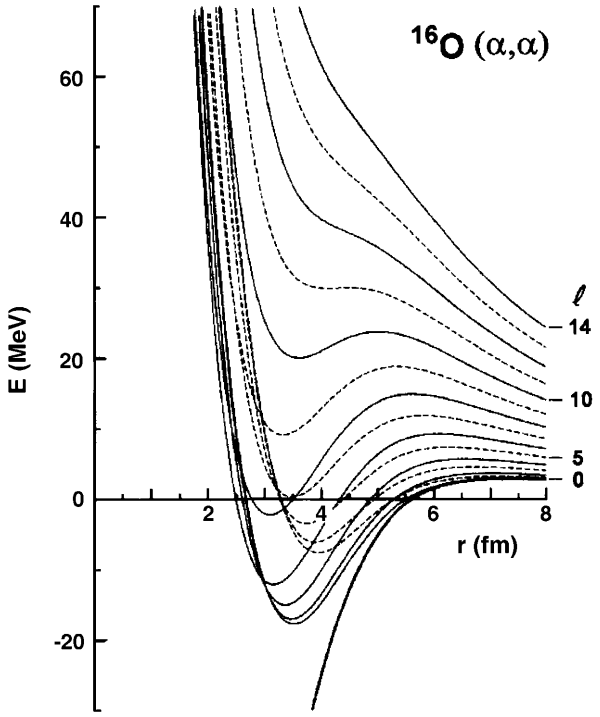

Fig. 1. Example of shallow local potentials for the interaction of α-particles with ^{16}O, fitting the elastic scattering and the resonances in ^{20}Ne, from ref. [21].

gives a very good description of the angular distributions of elastic scattering as well as of some states of ^{20}Ne. In this nucleus the ground state and the excited bands exhibit strong α-cluster structure, which are well reproduced in the cluster model. The corresponding local shallow potential, which is l-dependent, is shown in fig. 1. These are obtained by using the supersymmetric transformation (introduced by Baye [22] in 1987) from deep potentials, as they are obtained in semi-microscopic models like the double-folding model [23,24]. A phenomenological analysis using the optical model and a form factor of (Wood-Saxon)-squared shape for the real potential has also been very successful in describing a large variety of angular distributions of $\alpha + {}^{16}$O scattering [24,25]. Inspecting fig. 1, we note that the even and odd parity potentials are different, and that there is an overall dependence on the angular momentum of these potentials (apart from the trivial dependence due the centrifugal term). The strong repulsion at small distances can be interpreted (similar to the case of the $\alpha + \alpha$ system) as being due to the Pauli principle acting at small distances in this system. With a small adjustment, these shallow local potentials can be used to describe bound states of ^{20}Ne as well as the corresponding resonances and scattering states [21].

The structure of the ^{20}Ne nucleus has also been discussed in the frame of the deformed Nilsson model, a discussion of this approach will be given in conjunction with the ^{21}Ne structure in sect. 4. It is well known that the intrinsic cluster structure of ^{20}Ne corresponds to an octupole deformation and thus no definite parity for the intrinsic

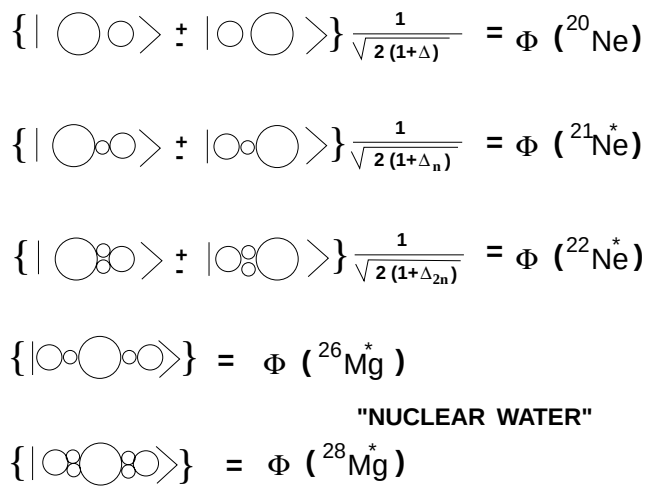

Fig. 2. Structure of states in $^{20\text{-}21}$Ne and $^{26\text{-}28}$Mg based on the $\alpha + {}^{16}$O cluster model with covalent valence neutrons. For intrinsically reflection asymmetric shapes, parity doublets with a possible splitting determined by the nonorthogonality Δ will be observed.

state can be defined. Such reflection asymmetric states have been discussed over many decades [18,26], and recently also for some other light nuclei like ^{18}O [27] and ^{19}F [28]. The projection K of the total angular momentum, is the relevant good quantum number. The states of good parity are obtained by forming linear combinations of two configurations with two possible signatures, as schematically shown in fig. 2. In this way two bands, "inversion doublets", of an instrinsic reflection asymmetric octupole with $K = 0$ and parities $\pi = (+ \text{and} -)$ are formed. The level scheme of ^{20}Ne is well known, there are two conspicuous bands with $K = 0^+$ and $K = 0^-$ (see fig. 4 below), which are also well described by the local $\alpha + {}^{16}$O potentials of fig. 1, as summarised in ref. [21]. The intrinsic asymmetric state of the ^{20}Ne would have produced *one band* with $I^\pi = J^{(-)^I}$ and with states of alternating parity, however, the nonorthogonality matrix element Δ, which connects the two configurations shown in fig. 2, is large in this case leading to a splitting of approximately 5 MeV between the bands with the two parities $\pi = (+)$ and $\pi = (-)$. The negative-parity band starts with a 1^- state at 5.787 MeV (there is no 0^- state allowed in this case). The higher-lying $K = 2^-$ band starting at 4.966 MeV is related to a single-particle excitation from the p-shell into the sd-shell, and the corresponding states are *not populated* in ^{16}O(^{7}Li, t) α-transfer reactions, whereas the cluster bands are strongly populated [29]. The higher bands (of natural parity) correspond to excitations from the sd-shell into the fp-shell, their cluster structure is also confirmed in α-transfer reactions [29]. Calculations based on the antisymmetrised molecular dynamics approach by Horiuchi [20] also show the pronounced clustering in the two parity split bands. It is actually much more pronounced in the $K = 0^-$ band.

In the cluster model, a transition between the two configurations can be defined, this can be a tunnelling process (similar to that of the nitrogen atom in the famous amonia molecule NH_3, with an instrinsic asymmetric configuration), or by a rotation by 180 degrees in the plane of the symmetry axis. This rotation can actually be visualised as being supported by the local $\alpha + {}^{16}$O potential. The explanation in the potential model is that the phase equivalent, local and shallow potentials are different for the two parities, which leads to the splitting of the two bands with $K = 0$. Other bands in ^{20}Ne are obtained in the cluster model by considering higher nodal wave functions in the relative motion [20,21].

2.2 Binding energies, the quasi-resonance condition in ^{21}Ne

I use the cluster model of ^{20}Ne to discuss states in ^{21}Ne with a molecular structure based on an additional covalent neutron. For this purpose, the neutron binding energies and the various thresholds are shown in fig. 3. The energy scale of the scheme is arranged in such a way, that the thresholds for $\alpha + {}^{16}\text{O} + x$ neutrons are aligned on a common horizontal line. From this line the binding of particular cluster states in the system can be read. The binding energy for the α-particle in ^{20}Ne is 4.730 MeV.

Figure 3 also shows the energies of the relevant single-particle states (or the resonances) for the two separate centres, namely for the decomposition into (^{5}He + ^{16}O) or into (α + ^{17}O). For the formation of the two-centre molecules with the structure ($\alpha + {}^{16}\text{O} + x$ neutrons), the states of the valence neutron in the systems ^{5}He and in ^{17}O must be considered. ^{5}He has an unbound state, a $p_{3/2}$ *resonance* at an energy of 890 keV (width 600 keV). The *ground state* of ^{17}O is a $d_{5/2}$ state with a binding energy of 6.7 MeV; this value is much larger than that for the resonant ground state in the (^{4}He + n) system and thus cannot be considered for a covalent binding situation; this

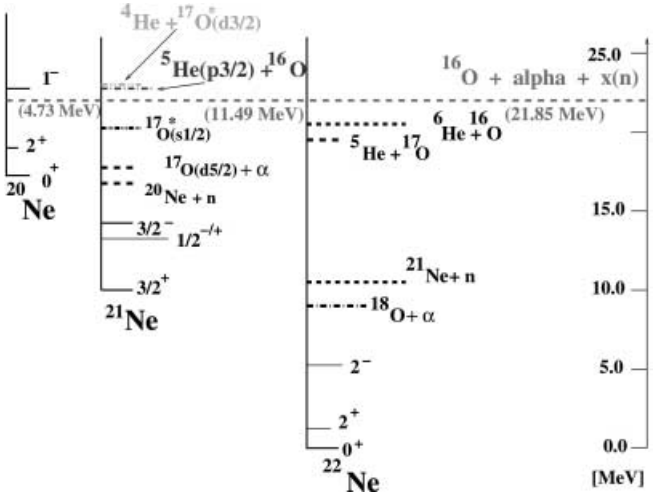

Fig. 3. Illustration of the thresholds (aligned to the same level) for the neon isotopes $^{20\text{-}22}$Ne in the $\alpha + (x$ neutrons) + ^{16}O cluster model. The J^π-values of band heads in $^{20\text{-}21}$Ne with their K quantum numbers are indicated.

would correspond to the case of an ionic configuration as in atomic molecules, a case which does not give binding effect in nuclear systems. The case of equal binding energies in the two separated fragments (which is trivially fulfilled for the case of identical cores) is the optimal condition for the covalent binding, which is called the *resonance condition* [30,31]. As indicated in fig. 3 it happens that a *quasi-resonance between the two states* is realised in the $\alpha + {}^{16}$O system for a covalent neutron with the mentioned $p_{3/2}$ resonance in ^{5}He and the $d_{3/2}$ resonance in ^{17}O at 0.941 MeV (width 96 keV). This fact will be used in the construction of the molecular wave function as explained below. It also happens that this resonance condition is identical to the well-known matching conditions in transfer reactions [30]. Another feature related to the dynamical matching aspect is the fact, that the transfer from a $d_{3/2}$ orbit to a $p_{3/2}$ orbit is favoured in quasi-stationary cases, because it corresponds to the "figure 8" trajectory [30]. In this circumstances also the tangential matching in the instrinsic motion of the valence nucleon is assured.

3 Molecular structures of the isotope ^{21}Ne

3.1 Molecular wave functions

In order to construct a molecular wave function in the cluster model for ^{21}Ne, we use some known principles of the method of linear combination of nuclear orbitals, the LCNO (known as LCAO in atomic molecules [1,5,9,16]). I define the total Hamiltonian so as to disregard the internal structure of the cores ^{16}O and ^{4}He and treat explicitly the interaction of the valence neutron with the two cores,

$$H_{\rm tot} = H_\alpha + T(\mathbf{r}_{\rm n\,\alpha}) + V_{\rm n,\alpha}(\mathbf{r}_{\rm n\,\alpha}) + T(\mathbf{r}_{\rm n\,^{16}O}) + H_{^{16}\rm O} + V_{\rm n,^{16}O}(\mathbf{r}_{\rm n\,^{16}O}) + T(\mathbf{R}) + V_{^{16}\rm O,\alpha}(\mathbf{R})\,. \quad (1)$$

The distance vector $\mathbf{R}$ is the coordinate between the two core centres. The coordinates for the neutron, $\mathbf{r}_{\rm n\,\alpha}$ and $\mathbf{r}_{\rm n\,^{16}O}$, point to the centres of the two clusters. The core-core potential already mentioned is $V_{^{16}\rm O,\alpha}(\mathbf{R})$, and the interaction of the neutron with the cores $V_{\rm n,\alpha}(\mathbf{r}_{\rm n\,\alpha})$ and $V_{\rm n,^{16}O}(\mathbf{r}_{\rm n\,^{16}O})$ is obtained by finding the solutions for the single-centre configurations. In dynamical calculations there occurs a serious problem to find solutions for such a two-centre system due to the recoil terms (due to $T(\mathbf{R})$) induced by the finite mass of the valence particle. This point will not be discussed here, see however refs. [2,5, 28]. The two-centre solutions can be constructed using the LCNO approach, which uses a linear combination of states in ^{17}O and ^{5}He (we use the two resonances in ^{17}O and ^{5}He, which are in a quasi-resonance condition as stated above), with the projection K of the spin as principal quantum number,

$$\Phi^K_{\rm LCNO}(\mathbf{R}, r_{\rm n}) = \frac{1}{\sqrt{2(1+\delta^K(\mathbf{R}))}} \times \big[a_{\rm n\,\alpha}\psi_\alpha\psi_{^{16}\rm O}\phi^K_{\rm n}(\mathbf{r}_{\rm n\,\alpha}, p_{3/2}) + (-)^{p1}a_{\rm n^{16}O}\psi_\alpha\psi_{^{16}\rm O}\phi^K_{\rm n}(\mathbf{r}_{\rm n^{16}O}, d_{3/2})\big]\,. \quad (2)$$

The coefficients $a_{\rm n\,\alpha}$ and $a_{\rm n\,^{16}O}$ will be almost equal in the case of resonance sharing of the valence particle, the factor $(-)^{p1}$ carries the sign of the two combinations, which form the new states, which replace the original single-centre states. For the two single centres the solutions are $\phi^K_{\rm n}(\mathbf{r}_{\rm n\,\alpha}, p_{3/2})$ and $\phi^K_{\rm n}(\mathbf{r}_{\rm n\,^{16}O}, d_{3/2})$, and the nonorthogonality $\delta^K(\mathbf{R})$ is given by their overlap, with $(\mathbf{r}_{\rm n\,\alpha} - \mathbf{R}) = \mathbf{r}_{\rm n\,^{16}O}$:

$$\delta^K(\mathbf{R}) = (-)^{p1}\int \phi^{*K}_{p_{3/2}}(\mathbf{r}_{\rm n\,\alpha})\phi^K_{d_{3/2}}(\mathbf{r}_{\rm n\,\alpha} - \mathbf{R})\mathrm{d}\mathbf{r}_{\rm n\,\alpha}\,. \quad (3)$$

The wave function, eq. (2), corresponds to a *reflection asymmetric* state and *no instrinsic parity* can be defined. As *quantum numbers* we have the *projections* on the symmetry axis: a) of the total angular momenta, K, and b) of the orbital angular momenta (Λ) of the valence particle denoted as in atomic physics, by σ for $\Lambda = 0$, and π for $\Lambda = 1$. States with total spin I and *good parity* Π are constructed by making the linear combinations (two signs (+) and (−) are possible!) with the *signatures* $= (-)^{I+K}$,

$$\Psi^{I,\Pi}_{KM}(\mathbf{R}, r_{\rm n}) = N(\Delta^K)\left[\Phi^K_{\rm LCNO}(\mathbf{R}, r_{\rm n})D^I_{MK}(\omega) + (-)^{I+K+p2}\Phi^K_{\rm LCNO}(\mathbf{R}, r_{\rm n})D^I_{M-K}(\omega)\right], \quad (4)$$

with

$$N(\Delta^K) = \frac{1}{\sqrt{2(1+\Delta^K)}}\,. \quad (5)$$

This construction is schematically shown in fig. 2, where the states of good parity for $^{20\text{-}21}$Ne result from a superposition of two reflection asymmetric structures. As illustrated in fig. 2, a new nonorthogonality term Δ may appear, which must be included into the normalisation $N(\Delta)$ as it was done in eq. (2). If we use the cited $d_{3/2}$ and $p_{3/2}$ orbitals, we obtain two possible values of the K quantum number $K = 1/2$ and $3/2$ for the molecular configurations, with two parities. These are the *parity doublets* for an asymmetric top with $K \neq 0$, as discussed by Herzberg [16] or by Bohr and Mottelson [17]. Note that the splitting of the parity doublets is now related *not* to the overlap $\delta^K(\mathbf{R})$ of eq. (3), but to the probability for a transition between the two shapes, which are generated by a rotation of 180° (or the two signatures), namely by Δ, as illustrated in fig. 2. For a completely rigid intrinsic structure, the two bands (*e.g.*, $K = 1/2^+$, $1/2^-$) will be almost degenerate ($\Delta \simeq 0$), such cases are known in heavy nuclei, for example in ^{225}Am and more cases are discussed in ref. [18]. The relation to the deformed Nilsson orbit is discussed by Leander and Sheline [32] and I will come back to this in sect. 4.

A different cluster model approach for ^{21}Ne has been pursued by Descouvement [33]. In this work ^{21}Ne is described by α-particle configurations directly related to the ^{17}O ground state, and these are superimposed by configurations where the neutron is bound to the ^{20}Ne ground state. In this way, the octupole structure and the intrinsically reflection asymmetric molecular structure proposed here is not obtained (actually also in this approach the description of the negative-parity states is rather unsatisfactory).

3.2 Level structure of ^{21}Ne

In this section an attempt is made of a complete spectroscopy of ^{21}Ne, namely to put the known states of ^{21}Ne into rotational bands, the negative-parity states are placed in parity doublets with intrinsic parity violation corresponding to the molecular structure discussed above. This implies a separation of states in ^{21}Ne into those related to the intrinsic octupole shape in ^{20}Ne, and the remaining states are then tentatively put into bands corresponding to the normal (quadrupole deformed) Nilsson orbit approach. This will correspond to a coexistence of octupole deformed states and quadrupole deformations. The spectroscopic studies for this mass range are typically more than 15-30 years old [34–38], however, quite detailed knowledge is available for many states and has recently been summarised for the heavier nuclei in the *sd*-shell by Roepke [36]. However, the odd parity states have usually been omitted in the discussion, because they go beyond the usual shell model scheme. In the molecular model based on the $(\alpha + {}^{16}\mathrm{O})$ cluster model with one neutron shared in the $p_{3/2}$ or $d_{3/2}$ resonances, we will now have two main bands as parity doublets with K-values of $1/2$ and $3/2$, and there appears a natural explanation for the negative-parity bands. The two $K = 1/2$ bands should exhibit very strong Coriolis decoupling structures, a fact which can be used to make configurational assignments. A second $K = 1/2^+$ shows no Coriolis decoupling effect (see fig. 4 and the discussion below).

The revision of the band structure of states in ^{21}Ne is supported by the fact that some of the original configuration assignments, which were used for the $K = 1/2$ bands, gave large contradictions with the predicted values of the decoupling parameters and the band structure in the experimental energy spectra appeared irregular. This is, in particular, the case for negative-parity states, which were usually not considered in detail [34–36]. Thus, a very conspicuous discrepancy is found in the calculated transition probability from the negative-parity state with $J^\pi = 1/2^-$ (at 2.78 MeV) to the $J^\pi = 3/2^+$ ground state. This $E1$ transition turns out to be retarded by more than three orders of magnitude, the lifetime with 110 ps! for this $1/2^-$ state is unusually long. The $E1$ decay into the ground state is strongly hindered, as noted in [34]: "A retardation of this extreme magnitude is difficult to explain with either the Nilsson or the shell models as already noted by Warburton *et al.* [37]". Using the molecular picture, the negative-parity states appear as partners in parity doublets, due to an intrinsic octupole shape and form a different class of states, with some possible configuration mixing in the positive-parity states.

For a complete spectroscopy, the following rotational bands should be present in ^{21}Ne:

a) Two parity doublets related to the octupole (molecular) shape, as bands with $K = 1/2$ and $3/2$, with $(-)$ and $(+)$ parity. b)The remaining states should be arranged into bands, which are due to "normal" *reflection symmetric* Nilsson model configurations. Here the low-lying states of ^{25}Mg are used as a guide-line, there the lowest states are [202,5/2],[211,1/2] and [202,3/2]. For the

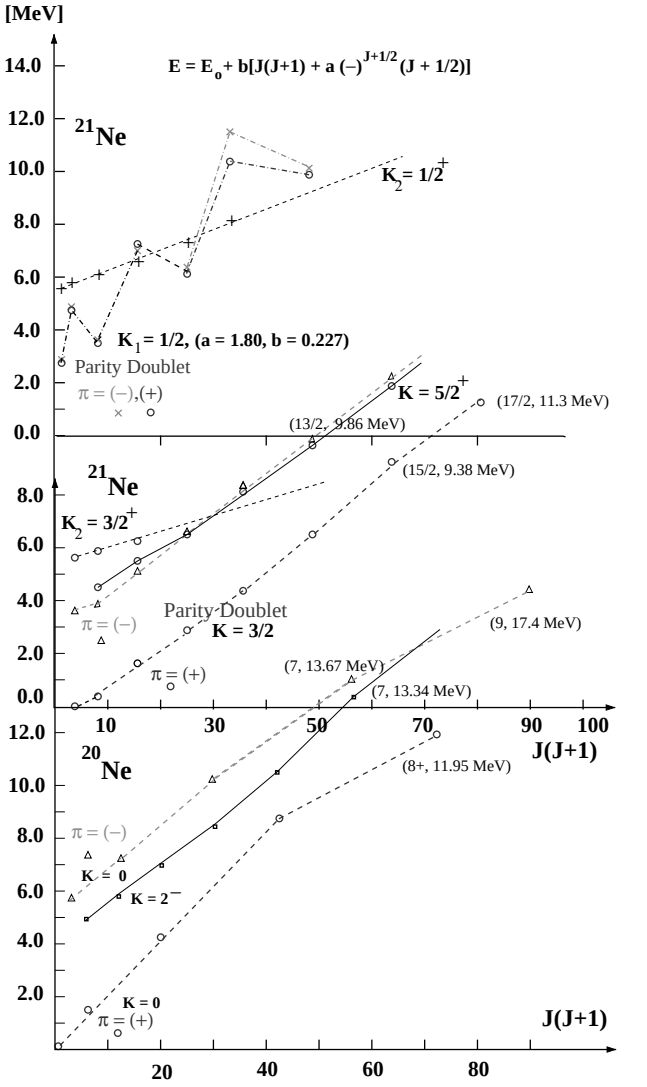

Fig. 4. Plot of the excitation energies of states in ^{20}Ne and ^{21}Ne showing molecular parity doublets forming rotational bands, as well as "normal"(quadrupole deformed) $K = 1/2$, $3/2$ and $5/2$ bands. This compilation places all low-lying negative-parity states in ^{21}Ne as belonging to parity doublets, as expected from signature splitting of the structures shown in fig. 2. The coefficients a and b are given for the band structure of the $K = 1/2$ parity doublet.

[220,1/2] and [211,3/2] Nilsson orbits we expect in addition two bands of positive parity with $K = 1/2, 3/2$, which may mix with the two positive-parity bands cited above, and, c) one [202,5/2], $K = 5/2$ band.

According to these expectations, the arrangement of states in fig. 4 is made differently as compared to ref. [35], actually in their work the negative-parity states are not discussed in detail, and in addition they state that: "the number of levels with positive and unassigned parity exceeds the shell model prediction for the number of positive-parity states in this excitation energy region". The presently proposed ordering into bands tries to incorporate the concepts described above and the knowledge on

the states of the Nilsson model as they appear in the low-energy spectrum of heavier *sd*-shell nuclei. Figure 4 shows the levels of ^{21}Ne arranged as parity doublets, which correspond to the suggested intrinsic molecular rotational band structure, plus the additional states.

The $K = 1/2$ bands for the molecular configuration are expected to show pronounced Coriolis decoupling patterns, which are not related to the deformed Nilsson model, but rather to the two-centre configuration (as in the case of the of ^{9,11}Be discussed in ref. [12]). For the $K = 1/2$ bands we have the unique possibility to use the Coriolis decoupling pattern to identify molecular cluster states. Such strong Coriolis decoupling patterns, as shown here for $K = 1/2$ bands, are also obtained for the case of ^{19}F in a cluster model study by Dufour and Descouvement [28]. The expression for the energy of the rotational band including the Coriolis decoupling parameter a and the inertia parameter b is given by

$$E(J) = E_0 + b\left[J(J+1) + a(-)^{J+1/2}(J+1/2)\right] . \quad (6)$$

The bands with $K = 1/2^+$ and $K = 1/2^-$, indeed, are almost degenerate and show a strong Coriolis decoupling. The figure shows that the moments of inertia are very similar to the two $K = 0$ bands in ^{20}Ne. For the $K = 3/2$ parity doublet, the proposed two bands are indicated in the middle frame, the $K = 3/2^+$ ground state band and a band with $K = 3/2^-$ starting at 4.3 MeV. These two bands appear with a slightly reduced splitting as compared to the $K = 0^{+,-}$ bands in ^{20}Ne. The other states are also compiled in fig. 4 so as to form bands with $K = 1/2$, $3/2$ and $5/2$, according to the usual Nilsson model. There appears a second $K = 1/2^+$ band without Coriolis coupling. The fact that the decoupling parameter a and the inertia parameter b are the same for the two members of parity doublets can be interpreted in the spirit of the work of Jolos and von Brentano [39,40] on parity split bands. For two stable octupole minima with $\beta_3 \neq 0$, the two bands are expected to have equal moments of inertia and the same Coriolis decoupling pattern, this is actually the case of ^{21}Ne. Following the same picture of refs. [39,40], the decay of the $1/2^-$ state to the ground state must be (as already mentioned) strongly hindered, because it will involve a change from a negative β_3 to a positive value. These two shapes are well separated by an internal barrier, which explains also the small energy splitting of the $K = 1/2$ doublet.

We can try to identify the intrinsic structure of the suggested molecular configurations for the $K = 1/2$ and $K = 3/2$ parity doublets. For $K = 1/2$ the orientation of the orbital angular momentum of the single-particle orbitals with $l = 2(d_{2/3})$ and $l = 1(p_{2/3})$ must have dominantly a σ bonding situation (projection on the symmetry axis $m = 0$). This configuration gives a strong concentration of the covalent neutron between the two cores. With this configuration we may indeed have a small transition probability measured by the nonorthogonality Δ as defined in fig. 2, the passage of the α-particle on the other side of the core is hindered. For the $K = 3/2$ case, a covalent orbit of the π type (l-projection, $m = 1$) must be involved, the neutron density distribution would then be concentrated outside of the symmetry axis and a splitting, as in the case of $K = 0$ bands in ^{20}Ne, can be expected. These two cases are schematically shown in fig. 5. The moments of inertia seem to be still dominated by the ^{20}Ne structure, a fact which can be explained from the shape of the local core-core potentials in fig. 1, which show a more pronounced minimum, and a cluster bound state, as opposed to the case of the α-α potential [21]. In the latter cases the moments of inertia in the isotopes $^{9\text{-}11}$Be do change with the configurations [12].

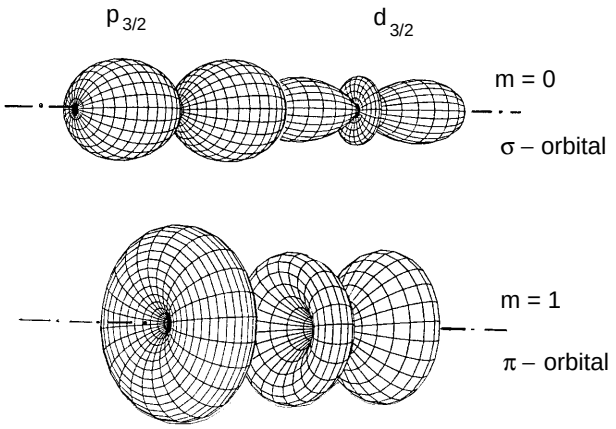

Fig. 5. Overlap of σ- and π-type orbitals consisting of $m = 0$ and $m = 1$ components of the $d_{3/2}$ and a $p_{3/2}$ configurations of the single centres. The former is responsible for the $K = 1/2$ parity doublet in ^{21}Ne, the latter for the $K = 3/2$ parity doublet. The corresponding bands are shown in fig. 4.

4 Relation to deformed shell model configurations

After compiling the four bands with $K = 1/2$ and $K = 3/2$, there are more positive-parity states; as already mentioned there would be at least three further bands with $K = 1/2$, $3/2$ and $5/2$ based on the $d_{5/2}$ and $s_{1/2}$ orbits *and a reflection symmetric deformed core*. Certainly, we must expect a mixing between states of the two configurations, although there may be a barrier in the corresponding shape variables between the classes of states. The number of states in particular those above 5 MeV excitation becomes quite large, however, the present approach gives a basis to explain all known states in the low-energy excitation region (up to 6–7 MeV). In the upper range of 6–12 MeV excitation energy the assignments of spin and parity to the states are uncertain. An attempt to place also the majority of the remaining known levels in terms of rotational bands is included in fig. 4.

We can define a second $K = 1/2^+$ band starting at an excitation energy of 5.68 MeV. States of this band do not show any Coriolis decoupling; I can identify this band with the [211]1/2 configuration, in fact a corresponding $K = 1/2$ band in ^{25}Mg starting at 0.585 MeV has a

vanishing Coriolis decoupling factor as cited on p. 284 in ref. [17]. The $K = 5/2$ band, also shown in fig. 4, is below the $K = 1/2$ band in close analogy to the situation in the cited ^{25}Mg nucleus. For the $K = 3/2$ band head I have chosen the state at 5.549 MeV slightly below the $K = 1/2$ band head, its moment of inertia appears larger. However, these assignments must be taken as conjectures, which can possibly be put on firmer basis by doing a complete spectroscopy for this nucleus with a large gamma-detector ball. Many of the states used do not have firm spin and parity assignments, and many states are above the particle threshold, their spins are partially inferred from their intensity from compound nucleus reactions like the ^{12}C(^{11}B, d)^{21}Ne reaction of ref. [41].

The deformation of ^{20}Ne, based on the concept of the deformed microscopic-macroscopic model [17,42], has been extensively discussed in the literature. In the latter work also axially asymmetric and reflection asymmetric cases are discussed. Octupole deformations and α-particle structure in light and heavy nuclei is produced by mixing orbits of opposite parity. In heavy nuclei, indeed, a very large configuration mixing across two major shells is needed to obtain the spectroscopic factors for α-particles [18]. If we want to discuss the structure of the parity doublets in ^{21}Ne based on the octupole deformation in the context of the deformed shell model, I have to discuss the coupling of the valence particle to the *reflection symmetric* deformed core. This will imply mixing of Nilsson orbits (characterised by the quantum numbers $[N, n_z, \Lambda, \Omega]$) with the same Λ and Ω, but differing in their principal quantum numbers defined by the increments given inside the brackets $[N+1, n_z(+,-)1]$. In this context, the members of the parity doublet should correspond to one single-particle orbit of mixed parity: this is obtained by a superposition of two Nilsson orbits with equal amplitudes and the same K-value, but differing in parity. Thus, for the reflection asymmetric case, the "strong" coupling between two orbits of equal amplitudes for the same values of Λ and $\Omega = K$ must occur. This phenomenon is related to the concept of hybridisation of valence orbitals, which is well known in atoms and is discussed for nuclear cases in refs. [5,11,8].

For the nuclear structure aspects I refer to the work of Leander and Sheline [32], where the strong and weak coupling scenarios are discussed and we use fig. 6 for the further discussion. For the $K = 1/2$ band, these two orbits differing by $[N+1, n_z(+,-)1]$ could be the [110,1/2] and [220,1/2] configurations. As shown in the Nilsson diagram of fig. 6, however, these orbits are rather far separated in energy for reasonable deformation values. Another alternative is the mixing of the [220,1/2] orbit with the [330,1/2] orbit, again this implies rather large deformations, as can be seen from the plots shown in fig. 6. As stated in many other cases, the nuclear structure aspects of strongly clustered configurations can, only with great difficulty, be obtained in an alternative (deformed shell model) basis, because large configuration mixing over many shells has to be invoked.

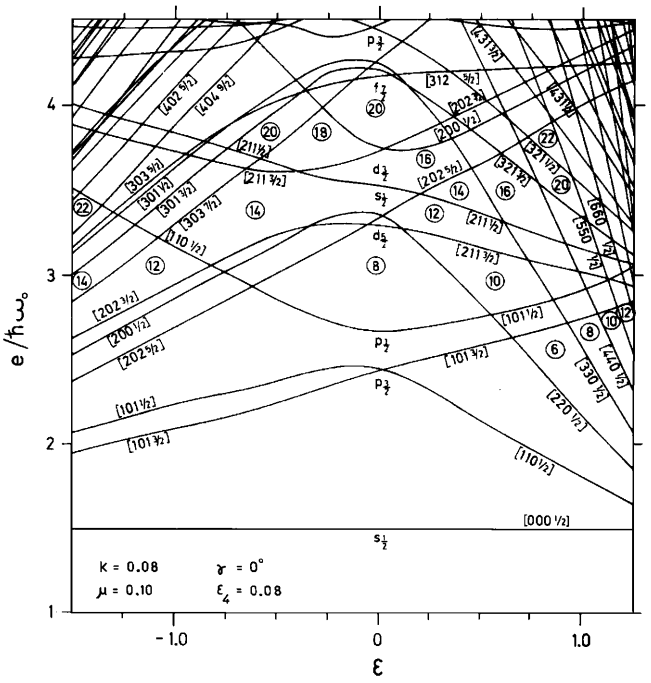

Fig. 6. The Nilsson diagram for the nucleon orbitals in the neon mass region, from ref. [32]. Note that the diagram is for $\epsilon_4 \neq 0$.

For the case of $^{20\text{-}21}$Ne a co-existence of cluster states with pronounced octupole deformation and normal Nilsson model configurations in the same excitation energy range must be expected. Such circumstances may be typical also for weakly bound systems, where cluster configurations appear close to and below the cluster decay thresholds. The case of ^{22}Ne will be discussed in later work, there the cluster states should appear at higher excitation, the thresholds being higher (see fig. 3). Due to the free combination of the two parity doublets in ^{21}Ne for two valence particles we can expect a "doubling of doublets" in ^{22}Ne. Actually, in recent work on resonances in the ^{18}O + ^{4}He system by V. Goldberg [43] such phenomenon of close doublets of states with the same parity has been observed.

5 Covalently bound molecules in the isotopes $^{26\text{-}28}$Mg and conclusions

Having established the existence of rotational bands forming parity doublets in ^{21}Ne, we may extrapolate the concept of covalent molecules to the (α + ^{16}O + α) systems. The corresponding cluster substructure in ^{24}Mg with $^{16}\text{O} + 2\,\alpha$ clusters is well known and usually shown in the Ikeda diagram in a slightly different way. I show in fig. 7 a reflection symmetric shape, where the two α-particles are arranged on two opposite sites of the central ^{16}O cluster. It is probably no surprise to find exactly such shapes in the work of Merchant and Rae [44,45] based on the cranked α-cluster model. Figure 2 and fig. 7 give a schematic illustration of such forms, which are equivalent to those shown in refs. [44,45]. The symmetric shapes

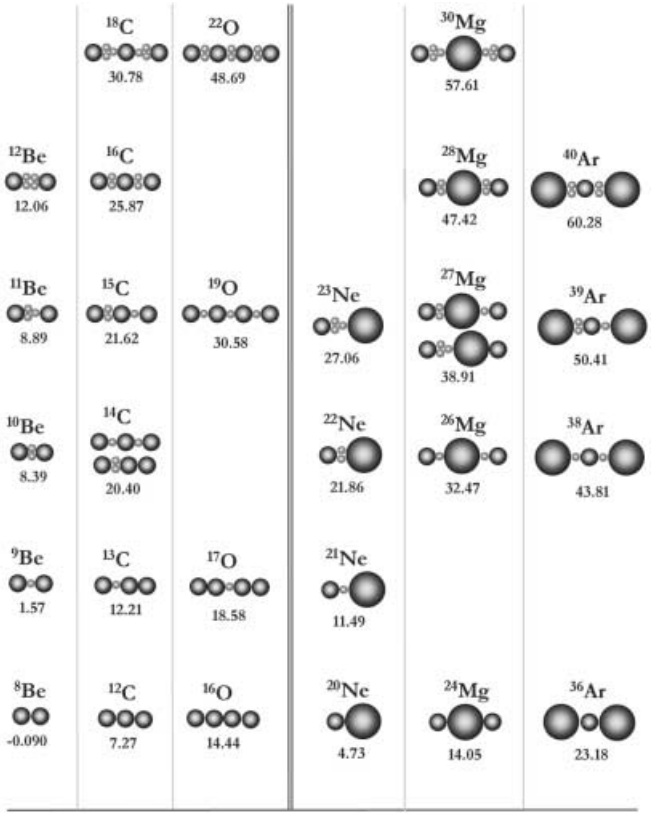

Fig. 7. Schematic illustration of the structure of molecular shape isomers in the neutron-rich isotopes of nuclei consisting of α and ^{16}O clusters, plus some covalently bound neutrons. For the odd mass isotopes each K quantum number gives rise to a parity doublet of bands due to the two signs of the signature. The splitting of these bands will be proportional to the probability to "tunnel" from one configuration to the other, given by the overlap Δ, as illustrated in fig. 2.

are expected at excitation energies well below the particle thresholds due to the properties of the $\alpha + {}^{16}$O potential (just like in ^{21}Ne), which is fairly attractive at its minimum. Such shapes can be described by a multipole expansion with even parity, and the states are expected to exhibit in addition to a large quadruple moment, large $l = 4$ and $l = 6$ (and higher) moments. Similar to the case of deformed nuclei in the rare earth region, these states should also be populated in inelastic scattering. Figure 7 shows some more of the expected shapes in analogy to the Ikeda diagram. The threshold energies for the separation into the cluster constituents plus neutrons are shown. Covalent binding in the case of σ and π orbitals is expected to produce quasi-bound (isomeric states) with energies comparable to the α-neutron bond of the $^{21\text{-}22}$Ne molecular states. This extended molecular Ikeda diagram gives a guide-line to future work for nuclear spectroscopy in light neutron-rich nuclei.

The author is indebted to H. Roepke for comments, and to A. Tumino for preparing fig. 7.

References

1. W. von Oertzen, Nucl. Phys. A **148**, 529 (1970); W. von Oertzen, W. Noerenberg, Nucl. Phys. A **207**, 113 (1973); W. von Oertzen, H.G. Bohlen, Phys. Rep. C **19**, 1 (1975).
2. B. Imanishi, W. von Oertzen, Phys. Rep. **155**, 29 (1987).
3. N. Bischof *et al.*, Nucl. Phys. A **490**, 485 (1988) and references therein.
4. J.Y. Park, W. Greiner, W. Scheid, Phys. Rev. C **21**, 958 (1980); A. Thiel, J. Phys. G **16**, 867-910 (1990).
5. B. Imanishi, W. von Oertzen, Phys. Rev. C **35**, 359 (1987); B. Imanishi, W. von Oertzen, *Proceedings of the Workshop on Heavy Ion Collisions at Energies near the Coulomb Barrier, Daresbury, 1990*, edited by M.A. Nagarajan, *IOP Conf. Ser.*, Vol. **110** (IOP, Bristol, 1990).
6. J.M. Sparenberg, D. Baye, B. Imanishi, Phys. Rev. C **61**, 054610 (2000).
7. M. Brenner, T. Loennroth (Editors), *TURKU Conference, International Conference on Nuclear and Atomic Clusters, EPS Topical Conference, Turku, Finnland, 1991* (Springer, Berlin, Heidelberg, 1992) p. 88.
8. W. von Oertzen, Th. Wilpert, B. Bilwes *et al.*, Z. Phys. A **353**, 373 (1996).
9. M. Seya, M. Kohno, S. Nagata, Prog. Theor. Phys. **65**, 204 (1981).
10. Y. Abe *et al.*, Prog. Theor. Phys. **49**, 800 (1973).
11. B. Imanishi, W. von Oertzen, Phys. Rev. C **52**, 3249 (1995).
12. W. von Oertzen, Z. Phys. A **354**, 37 (1996); **357**, 355 (1997); Nuovo Cimento A **110**, 895 (1997).
13. H. Horiuchi *et al.*, *Proceedings of the International Conference on Atomic and Nuclear Clustering, Santorini, 1993*, edited by W. von Oertzen, G.S. Anagnastatos (Springer, 1995); Z. Phys. A **349**, 142 (1994).
14. Y.K. Kanada-En'yo, H. Horiuchi, A. Ono, Phys. Rev. C **52**, 647 (1995); **56**, 1844 (1997).
15. Y.K. Kanada-En'yo, H. Horiuchi, A. Dote, J. Phys. G **24**, 1499 (1998).
16. G. Herzberg, *Molecular Spectra and Molecular Structure* in *Spectra of Diatomic Molecules*, Vol. **I** (D. Van Nostrand Company Inc., Princeton, 1950) p. 129.
17. A. Bohr, B. Mottelson, *Nuclear Structure*, Vol. **II** (Benjamin Inc., Reading, Ma, 1975).
18. P.A. Butler, W. Nazarewicz, Rev. Mod. Phys. **68**, 350 (1996).
19. K. Ikeda, N. Tagikawa, H. Horiuchi, Prog. Theor. Phys. (Jpn.) Suppl. 464 (1968).
20. H. Horiuchi, K. Ikeda, Y. Suzuki, Prog. Theor. Phys. (Jpn.) Suppl. **52**, chapt. 3 (1972).
21. S. Ohkubo *et al.*, Prog. Theor. Phys. Suppl. **132**, 1-133 (1998).
22. D. Baye, Phys. Rev. Lett. **58**, 2738 (1987).
23. B. Buck, C.B. Dover, J.P. Vary, Phys. Rev. C **11**, 1803 (1975).
24. H. Abele, G. Staudt, Phys. Rev. C **47**, 742 (1993).
25. F. Michel, *Proceedings of the Fifth Interantional Conference on Clustering Aspects in Nuclear and Subnuclear Systems, Kyoto, Japan, 1988*, edited by K. Ikeda (Physical Society of Japan, 1989) p. 65.
26. H.J. Krappe, U. Wille, Nucl. Phys. A **124**, 641 (1969).
27. G. Reidemeister, F. Michel, Phys. Rev. C **47**, R1846 (1993).
28. M. Dufour, P. Descouvement, Nucl. Phys. A **672**, 153 (2000) and references therein.

29. N. Anantaraman, H.E. Gove, R.A. Lindgren et al,, Nucl. Phys. A **313**, 445 (1979) and references therein.
30. L.J.B. Goldfarb, W. von Oertzen, in *Heavy Ion Collisions*, edited by R. Bock, Vol. **1** (North Holland, Amsterdam, 1980).
31. V.Yu. Denisov, J. Nucl. Phys. (Soviet. Phys.) **39**, 825 (1984).
32. G. Leander, R.K. Sheline, Nucl. Phys. A **413**, 375 (1984).
33. P. Descouvement, Phys. Rev. C **48** 2746 (1993).
34. A.A. Pilt, R.H. Speak, R.V. Elliott *et al.*, Can. J. Phys. **50**, 1826 (1972).
35. A. Hoffmann, P.Betz, H. Roepke, B.H. Wildenthal, Z. Phys. A **332**, 289 (1989).
36. H. Roepke, Nucl. Phys. A **674**, 95 (2000).
37. E.K. Warbuton, E.O. Olness *et al.*, Phys. Rev. C **3**, 2344 (1971).
38. C. Rolfs *et al.*, Nucl. Phys. A **167**, 449 (1971).
39. R.V. Jolos, P. von Brentano, Phys. Rev. C **49**, R2301 (1994).
40. R.V. Jolos, P. von Brentano, Nucl. Phys. A **587**, 377 (1995).
41. H. Rosner, Dr. Thesis, MPI-Heidelberg, 1976.
42. G. Leander, S.E. Larsson, Nucl. Phys. A **239**, 93 (1975).
43. V. Goldberg, *Contribution to the Workshop DREB (Direct Reactions with Exotic Beams) Orsay, July, 2001*; private communication.
44. S. Marsh, W.D. Rae, Phys. Lett. B **180**, 185 (1986).
45. J. Zhang, W.D.M. Rae, A.C. Merchant, Nucl. Phys. A **575**, 61 (1994).